Molecular Dynamics (MD) Calculation on Ion Implantation Process with Dynamic Annealing for Ultra-shallow Junction Formation

Ohseob Kwon, Kidong Kim, Jihyun Seo, and Taeyoung Won

Department of Electrical Engineering, School of Engineering, Inha University
253 Yonghyun-dong, Nam-gu, Incheon, Korea 402-751, E-mail: kos@hsel.inha.ac.kr

ABSTRACT

In this paper, we report a molecular dynamics (MD) simulation of the ion implantation for nano-scale devices with ultra-shallow junctions. In order to model the profile of ion distribution in nanometer scale, the molecular dynamics with a damage model has been employed while the kinetic Monte Carlo (KMC) diffusion model was used for the dynamic annealing between cascades. The distribution of dopants during the ion implantation was calculated from the MD approach. The calculation has been performed for B with energies down to 100eV and dose 1 10^{14} ions/cm^2. The B, As, and Ge implant has been simulated with the energies of 0.5, 1, 2, 4, 8, and 16 keV and with dose 1 10^{14} ions/cm^2 into Si <100>, respectively.

Keywords: molecular dynamics, kinetic monte carlo, ion implantation, diffusion, dynamic annealing

1 INDRODUCTION

Ion Implantation induced dopant and damage distribution is of major process among the silicon technology. A need for predictive range profile in the area of ion implantation modeling puts much emphasis on accurate physical modeling of the implant process for nano-scale devices. Monte Carlo methods based on BCA (Binary Collision Approximation) have been used in the past with describing many physical mechanisms. However, although the multiple interactions must be taken into account for ultra-low energy ion implantation, BCA has shortcomings because the basic assumption is the binary collision in which many factors for ion implantation is difficult to be illustrated realistically. Despite molecular dynamics (MD) approach requires too excessive computation time, an accurate distribution of dopants can be expected quite during the ion implantation can be calculated by using appropriate functions for inter-atomic potentials [1,2]. In addition, it is not clear whether ion-beam induced annealing plays a role under ion implantation. In this paper, we report our study on the ion implantation process for ultra-low energy by using MD method for describing dynamic annealing for dopant redistribution and defect recombination within a recoil cascade.

2 SIMULATION MODEL

In order to model the ultra shallow junction, a recoil interaction approximation was applied for ion implantation (RIA). The Ziegler-Biersack-Littmark (ZBL) potential model, Eq. (1), has been used for the interaction among atoms. In order to model the electronic stopping power, the density functional theory by Echenique *et al* [3] was implemented in this work. Furthermore, the Firsov model was employed in order to model the energy loss during the inelastic collisions [4].

$$E_{ZBL} \quad V(r_{ij}) \quad \frac{Z_1 Z_2 e^2}{R_{ij}} \sum_{k\ 1}^{4} c_k \exp\left(\ d_k \frac{r_{ij}}{a} \right), \qquad (1)$$

The distribution of the concentration of dopants was calculated using the environment-dependent inter-atomic potential (EDIP). The critical step is performed such as following steps for the simulation of ion implantation process using MD; a) the initial configuration including position and velocity of recoil atom is defined. b) the potential is calculated between recoil atom and lattice atoms. Finally, c) the next configuration is calculated.

The lattice atoms may be annealed by ion bombardment during ion implantation. The ion-beam induced annealing affects dopant redistribution and defect recombination within a recoil cascade. The dynamic annealing during ion implantation is effective as much as annealing after implantation. The dynamic annealing may be explained the defect recombination within a recoil cascade, the stabilization of defects when overlapped by subsequent collision cascades, and the results in a lower overall number of defects. For the consideration of dynamic annealing during ion implantation and an accurate model for diffusion of intrinsic point defects (I, V) and impurities (B) in ion-implanted silicon, our approach is based upon the coupled calculation of MD and KMC. From the atomic distribution during the ion implantation from MD simulation, the dynamic development (hopping) of impurities and defects are calculated using KMC. The KMC simulation is interactively performed with the results of the MD simulation.

In this type of KMC model, point defects and dopants are treated at an atomic scale while they are considered to diffuse in accordance with the reaction rates, which are

given as input parameters [5]. The input parameters can be obtained from either first-principles calculations or classical MD simulation, or experimental data. Especially, the formation of clusters and extended defects, which usually control the annealing kinetics after ion implantation, should be minimized in the range of low dose in an effort to create dilute concentrations of I and V. Therefore, a simple kick-out mechanism has been tested and a good agreement with the experimental data [6] was verified in this condition. However, a more recent model, interstitialcy mechanism, is preferred when compared to the traditional kick-out mechanism by *ab initio* molecular dynamics [7].

An atomistic diffusion mechanism involving fast-migrating intermediate species of the form is proposed. The reactions $X_s + I \Leftrightarrow X_m$, and $I + V \Leftrightarrow 0$ are essentially diffusion limited, with capture radius of second neighbor atomic length (3.84Å) and direction of particle migration is limited to six neighbor sites. Here, X_s is the immobile substitution impurity, which through reaction with a self-interstitial (I) forms a fast-migrating species X_m, which diffuse at a rate D_m. The diffusion rate is form in Arrhenius type ($D_0 \exp(-E_{act}/KT)$). KMC simulations are performed by using the damage profiles and defects distribution from the MD simulations. The KMC is an event-driven technique, i.e., simulate events at random with probabilities according to the corresponding event rates. In this way, it self-adjusts the reasonable time step as the simulation proceeds.

3 RESULTS AND DISCUSSION

Fig. 1 shows the calculation results for B implant with the energies of 1, 3, and 5keV with the dose of 1 10^{14}ions/cm^2 into Si<100>. The tile and rotation angle is 0'. In case of 1keV, the peak is shown near the surface to the energy of 5keV, but on the other hand the end of range is deeper than the energy of 1keV. The mean range of ion implantation with the energy of 1keV is 27 Å because the most part of implantation energy is lost due to the bombardment with surface atoms. The max range of ion implantation with the energy of 5keV is 870 Å, which is about 4.3 times deeper than the ion implantation with the energy of 5keV. The difference may be explained that the surface is more amorphized, followed by the more energy loss than the ion implantation with the energy of 1keV. In case of Fig. 2, B implant with the energy of 5keV with the dose of 1 10^{14}ions/cm^2 and 1 10^{15}ions/cm^2 into Si<100>, small dose dependence is only shown. However, if there is more dose difference, the results similar with Fig.1 may be shown.

Fig. 3 shows the simulation results for B implantation with for energies down to 100eV below 1keV, and Fig. 4 shows the mean range and the sputter energy per ion. In Fig.3, the most atoms are within the range of 100Å. The differences of peak values are shown as the implantation energy increases. In Fig. 4, the linear difference of mean range below the energy of 1keV is shown as the implantation energy increases. The effect of surface amorphization is little more than above the range of implantation energy of 1keV.

Fig.5, 6, and 7 were performed on a Si target of <110> crystal direction at a temperature of 300K. Dopants and damage profiles were simulated for B, As, and Ge ions with the dose of 1 10^{14} ions/cm^2. Fig.5 shows the simulation results with the energy of 0.5, 1, 2, 4, 8, 16keV B implant. In the case of Fig. 6 and Fig. 7, the implant ions are As and Ge, respectively. As boron ion dose increases, local damage accumulation affects the dopant distribution more appreciably in the case of ultra-low energy ion implantation. In other words, the channeling tail drops very steeply with the increase of the amount of dose. In the case of As, the channeling tail drops very steeply with depth. This phenomenon is due to the large atomic mass of As.

Fig. 8 shows the simulation results with the energy of 8keV B implant into Si after 500 and 4,000 B ions. The KMC simulation is performed by using 3D dopant distribution and defects. Fig. 9 shows the result of B implantation with/without the dynamic annealing. In Fig. 6, the mean range with/without the dynamic annealing is 719.4 ±13.3 Å and 241.8±4.4 Å, respectively. The peak value is decreased and the concentration at the tail increases due to the effect of dynamic annealing. Table 1 illustrates the parameters of EDIP for Si.

4 CONCLUSIONS

The simulation of low-energy ion implantation for B, As, and Ge has been performed to energy range as low as 100eV by using the MD method. In case of B implantation, the characteristics of the mean range, max range, and sputtered atoms is investgated, followed by showing the difference of simulation results as the range of implantation energy. In the below range of implantation energy of 1keV with dynamic annealing, the more accurate potential for describing the mechanism of ultra-low energy ion implantation may be needed.

ACKNOLEDGEMENT

This work was supported partly by the Ministry of Information & Communication (MIC) of Korea through Support Project of University Information Technology Research Center (ITRC) Program supervised by IITA (Institute of Information Technology Assessment).

REFERENCES

[1] J. Nord, *et al,* Phys. Rev. B (2002).

[2] J. Peltola *et al*., Nucl. Instr. Meth. Phys. Res. B, (2002).

[3] P. M. Echenique *et al*., Appl. Phys. A 71, 503 (2000).

[4] P. Keblinski *et al,* Phys. Rev. B 66, 4104 (2002).

[5] Martin Jaraiz, Atomistic simulations in Materials Processing.

[6] N.E.B. Cowern *et al*, Phys Rev Lett Vol 69 (1992).

[7] Paola Alippi *et al*, Phys Rev B, Vol 64 (2001).

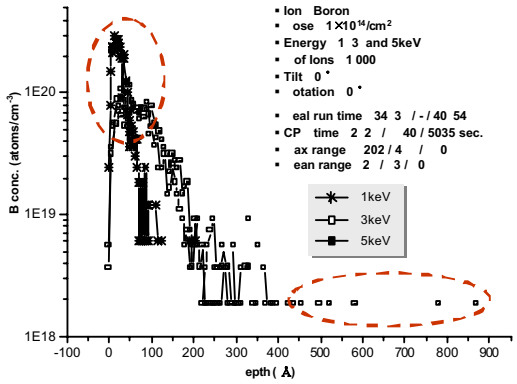

Fig. 1 A plot showing the simulation results for B implant with the energies of 1, 3, and 5keV and the dose of 1 10^{14} ions/cm^2 into Si<100>.

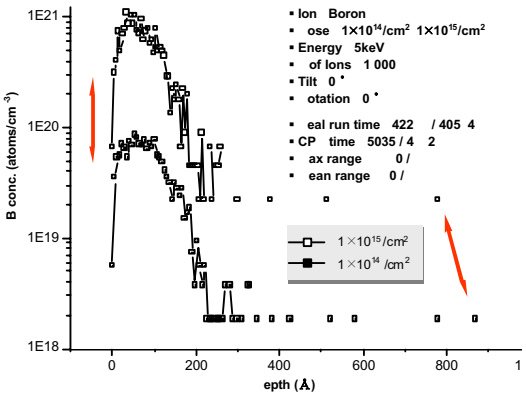

Fig. 2 A plot showing the simulation results for B implant with the dose of 1 10^{14} ions/cm^2 and 1 10^{15} ions/cm^2 and the energy of 5keV into Si<100>.

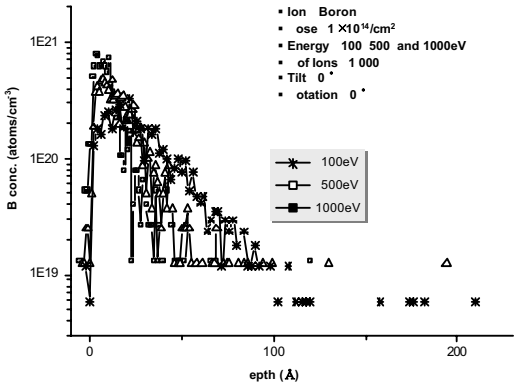

Fig. 3 A plot showing the simulation results for B implant with the energies of 100, 500, and 1,000eV and the dose of 1 10^{14} ions/cm^2 into Si<100>.

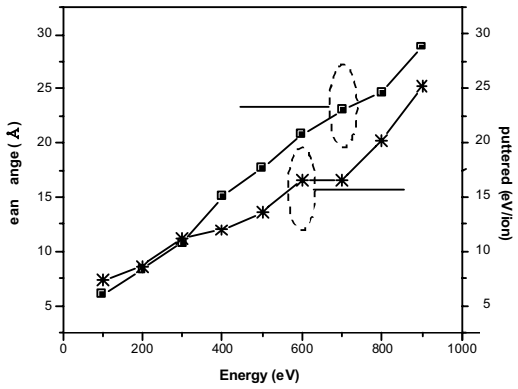

Fig. 4 A plot showing the mean range and the sputtered atoms for B implant with the energies of 100, 500, and 1,000eV and the dose of 1 10^{14} ions/cm^2 into Si<100>.

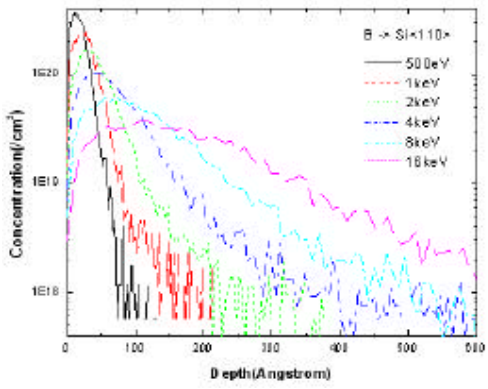

Fig. 5 A plot showing the simulation results for B implant with the energies of 0.5, 1, 2, 4, 8, and 16keV and the dose of 1 10^{14} ions/cm^2 into Si<110>.

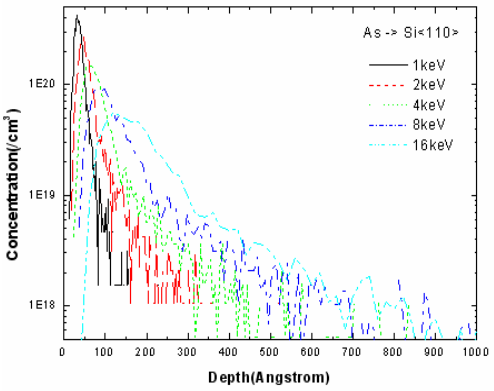

Fig. 6 A plot showing the simulation results As implant into Si with energies of 1, 2, 4, 8, and 16keV and the dose of 1 10^{14}ions/cm^2.

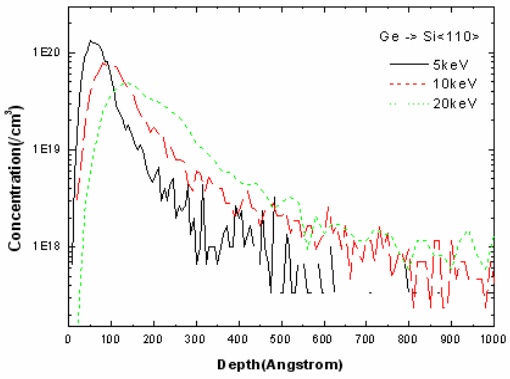

Fig. 7 A plot showing the simulation results for Ge implant into Si with the energies of 5, 10, and 20keV and the dose of 1 10^{14}ions/cm^2.

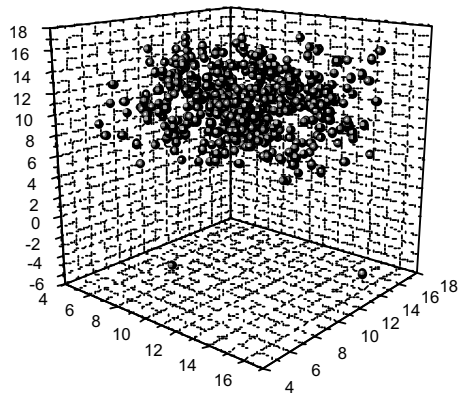

(a)

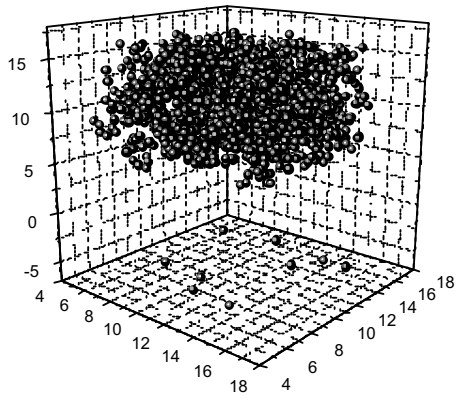

(b)

Fig. 8 Plots showing the simulation results with the energy of 5keV B implant into Si; (a) after 500 B ions and (b) after 4,000 B ions.

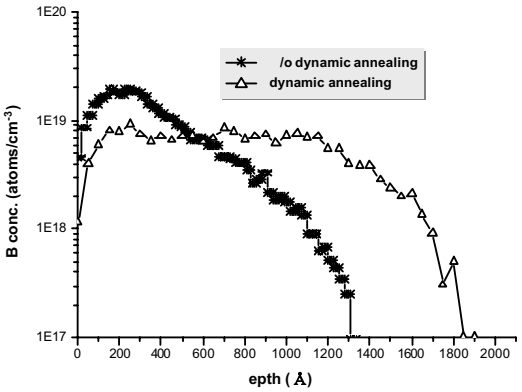

Fig. 9 A plot showing the simulation result with the energy of 5keV and the dose of 1 10^{14}ions/cm^2 B implant into Si with/without the dynamic annealing.

Table 1. Parameters of EDIP for Si.

Parameter	Value	Parameter	Value
A	7.9821730 eV	?	1.1247945 Å
a	3.1213820 Å	μ	0.6966326
	1.4533108 eV	?	1.2085196
Q_0	312.1341346	s	0.5774108 Å
	3.1083847	?	0.2523244
B	1.5075463 Å	ß	0.0070975
c	2.5609104 Å		